OXFORD

ORIGINAL MANUSCRIPT

Beneficial effects of the naturally occurring flavonoid silibinin on the prostate cancer microenvironment: role of monocyte chemotactic protein-1 and immune cell recruitment

Harold Ting[1], Gagan Deep[1,2], Sushil Kumar[1], Anil K. Jain[1], Chapla Agarwal[1,2] and Rajesh Agarwal[1,2,*]

[1]Department of Pharmaceutical Sciences, Skaggs School of Pharmacy and Pharmaceutical Sciences and [2]University of Colorado Cancer Center, University of Colorado Denver Anschutz Medical Campus, 12850 East Montview Blvd, V20-2118, Box C238, Aurora, CO 80045, USA

*To whom correspondence should be addressed. Tel: +1 303 724 4055; Fax: +1 303 724 7266; Email: rajesh.agarwal@UCDenver.edu

Abstract

Tumor microenvironment plays an essential role in prostate carcinogenesis and offers novel opportunities to prevent and treat prostate cancer (PCA). Here, we investigated the ability of cancer-associated fibroblasts (CAFs) to promote PCA progression, and silibinin efficacy to target this response. We collected conditioned media from CAFs treated with vehicle or silibinin, and labeled as control conditioned media (CCM) or silibinin-treatment conditioned media (SBCM), respectively. Next, we characterized the effect of CCM and SBCM treatment in several PCA cell lines (RWPE-1, WPE-1 NA-22, WPE-1 NB-14 and PC3). Result showed that compared with SBCM, CCM significantly reduces E-cadherin expression and increases invasiveness and clonogenicity in PCA cells. Further molecular studies identified monocyte chemotactic protein-1 (MCP-1) as the key component of CCM that promotes PCA invasiveness, whereas silibinin treatment strongly reduced MCP-1 expression in CAFs by inhibiting the DNA-binding activity of MCP-1 transcriptional regulators—nuclear factor-kappaB and AP-1. *In vivo*, silibinin feeding (200 mg/kg body weight) strongly reduced TRAMPC1 allografts growth (by 68%) in syngeneic C57Bl/6 mice. TRAMPC1 tumor analysis showed that silibinin reduced MCP-1 and CAFs' biomarkers (fibroblast activation protein, α-smooth muscle actin, transforming growth factor beta 2, vimentin etc.) and significantly modulated the recruitment of immune cells in the tumor microenvironment. Similar inhibitory effects of silibinin on MCP-1 and immune cells recruitment were also observed in TRAMP PCA tissues with reported silibinin efficacy. Overall, our data suggest that silibinin can target CAF-mediated invasiveness in PCA by inhibiting MCP-1 secretion. This, in turn, was associated with a reduction in immune cell recruitment *in vivo* along with a marked reduction in tumor growth.

Introduction

Classically, the microenvironment of a tumor has been seen as a passive bystander in carcinogenesis; the growing tumor being the only active player, progressively overcoming molecular and cellular barriers through various stages of cancer development (1). In contrast to this traditional view, the tumor microenvironment has recently been recognized as an active participant in the development of a tumor contributing to many of the hallmark properties of cancer such as promoting angiogenesis and proliferative signals while inhibiting apoptosis and growth suppressors, along with other dysfunctional activities (2–6). The tumor microenvironment may in fact be a critical and necessary element to cancer progression, and therefore, understanding this component would provide new targets for novel treatments necessary to address the growing burden of cancer worldwide (7–9).

Abbreviations

PCA	prostate cancer
CAFs	cancer-associated fibroblasts
CCM	control conditioned media
SBCM	silibinin-treatment conditioned media
MCP-1	monocyte chemotactic protein
DMSO	dimethyl sulfoxide
ELISA	enzyme-linked immunosorbent assay
TGFβ2	transforming growth factor beta 2
TRAMP	transgenic adenocarcinoma of the mouse prostate
CXCL1	chemokine (C–X–C motif) ligand 1
NK-κB,	nuclear factor-kappaB

Within the tumor microenvironment, fibroblasts represent the most numerous cellular element (10). Normally, fibroblasts are quiescent, but can be activated in the case of an injury to differentiate into myofibroblasts (11). It is this last activity combined with their large number that highlights their importance to the tumor microenvironment. These fibroblasts can be thought of as cancer associated, residing in close proximity to the expanding borders of a growing tumor. Most importantly, these cancer-associated fibroblasts (CAFs) are irreversibly and constitutively activated, and unlike myofibroblasts activated in response to a wound, they are not subject to programed cell death allowing for their continued activity (12,13). In fact, their presence has been associated with poor prognosis in several cancer types (14–16).

In this context, we have recently identified the capacity of prostate cancer (PCA) cells to alter the phenotype of naive human fibroblasts into one similar to CAFs isolated from clinical resections of PCA patients (17). In other words, PCA cells could 'educate' nearby healthy fibroblasts to acquire a CAF phenotype. In the present study, we now turned to investigate the capacity of CAFs to alter the phenotype of PCA cells. We sought to identify if CAFs could induce PCA growth and progression, as well as to elucidate the molecular mechanism underlying our observations. Toward these goals, we used PCA patient's CAFs to formulate CAF conditioned media (labeled as CCM). This provided a means to replicate the transmission of activating signals from CAFs to nearby cells, while also allowing for the specific treatment of CAFs in isolation. In parallel, we investigated whether we could target CAFs-induced activity in PCA cells with the natural compound silibinin, which has shown broad anti-cancer efficacy several cancer models, including PCA, inhibiting growth, angiogenesis, invasion and metastasis, while promoting apoptosis (18–26). CAFs were treated with silibinin, and these cells were used to 'condition' media that was labeled silibinin conditioned media (SBCM). In addition, we investigated whether silibinin could directly interfere with CAF-mediated activation of PCA cells. We also examined the potential of CAF–PCA cell activation (as well as its inhibition by silibinin) within mouse models to recreate the clinically relevant conditions of the tumor microenvironment found in an organism. This would also allow for the introduction of immune cells to our PCA tumor model. This was an important consideration as the chronic inflammation associated with dysregulated leukocyte recruitment to tumors has been linked to cancer progression (4,27). Our results indicate that CAFs do in fact have the capacity to activate PCA cells that we found to be dependent on monocyte chemotactic protein-1 (MCP-1), and this effect could be inhibited by silibinin treatment of either CAF or PCA cells. Consistent with the defined role of MCP-1 in leukocyte recruitment, in our mouse models, we identified significant immune cell recruitment and fibroblast activation, which were inhibited by silibinin treatment.

Materials and methods

Reagents and cell culture

All cell lines (RWPE-1, WPE-1 NA-22, WPE-1 NB-14 and PC3) and Dulbecco's modified Eagle's media were from ATCC (Manassas, VA). All cell lines were authenticated according to vendor sources and used within 6 months of receipt or resuscitation. RWPE-1, WPE-1 NA-22, WPE-1 NB-14 and PC3 cell lines represent the non-neoplastic (immortalized), prostatic intraepithelial neoplasia, adenocarcinoma and hormone-refractory metastatic stage of the PCA, respectively. These cell lines cover the full spectrum of the PCA disease, and therefore, they were used for the proposed studies. PC3 cells were re-authenticated by short tandem repeat profile testing on 24 July 2015 at the BDC BioResources Core Facility, University of Colorado Denver. MCDB105 media was from Sigma–Aldrich (St Louis, MO). CAFs were generously provided by Dr Scott D.Cramer as described previously (17). Silibinin stock solution was prepared in dimethyl sulfoxide (DMSO). An equal amount of DMSO was present in each treatment; DMSO concentration did not exceed 0.1% (v/v) in any treatment.

Conditioned media

Control conditioned media (CCM) and SBCM samples were formulated by incubating CAFs in MCDB105 media (10% fetal bovine serum) with DMSO vehicle or silibinin (90 μM), respectively. After 72 h, cells were washed twice with phosphate-buffered saline and then incubated for 48 h in low serum MCDB105 media (0.5% fetal bovine serum) without vehicle or silibinin. This conditioned media was then collected and labeled 'CCM' or 'SBCM' based on initial treatment. Cells were counted to normalize conditioned media volume against cell number. This experimental protocol and the silibinin dose used were based upon our earlier published similar studies (17,28).

Immunofluorescence confocal microscopy

Cells were grown on cover slips and incubated in the appropriate treatment as indicated. Cells were treated for 24 h, then fixed and blocked. Cells were then incubated with anti-E-cadherin primary antibody (Cell Signaling, Danvers, MA). Cells were then incubated with Alexa Fluor 555-tagged secondary antibody from Molecular Probes (Eugene, OR) along with 4′,6-diamidino-2-phenylindole. Cell images were captured at ×600 magnification on a Nikon inverted confocal microscope using 561/405 nm laser wavelengths to detect E-cadherin (red) and 4′,6-diamidino-2-phenylindole (blue) emissions, respectively. Fluorescence intensity was quantified using Image J software.

Invasion assay

Invasion assay was performed using Trans-well chambers from BD (Corning, NY) as per vendor's protocol. Briefly, bottom chambers were filled with appropriate treatment as indicated, and top chambers were seeded with 100 000 cells (WPE-1 NA-22 and WPE-1 NB-14) or 25 000 cells (PC3) in media (with 0.5% fetal bovine serum). After 18 h of incubation, non-invasive cells were removed and invasive cells were fixed, stained and mounted. Images were captured using Cannon Power Shot A640 camera on a Zeiss inverted microscope, and total number of invasive cells was counted.

Clonogenic assay

Cells were cultured on six-well plates (5×10^2 per well), and every 48 h, fresh media and appropriate treatment were added. On eighth day, cells were washed, fixed and stained. Colonies with >50 cells were scored. Photomicrographs were captured using Canon Power Shot digital camera.

Cytokine, chemokine and enzyme-linked immunosorbent assays

CCM and SBCM were analyzed by cytokine array and MCP-1 enzyme-linked immunosorbent assay (ELISA) (both from R&D, Minneapolis, MN) per vendor's protocols. For the MCP-1 ELISA, regression curves from known standards were used to quantify the resultant optical density as concentrations of MCP-1. Band intensity was quantified using Image J software.

Real-time PCR

CAFs were incubated with appropriate treatment, and cells were collected and lysed. Total RNA was then isolated first strand cDNA prepared per vendor's protocols (Qiagen, Germantown, MD), with concentration and purity confirmed by NanoDrop 2000 spectrophotometer (Thermo Scientific). For quantitative reverse transcription–PCR analysis, human-specific primers for MCP-1 (Qiagen, Germantown, MD): forward primer (5′-AAGATCTCAGTGCAGAGGCTCG-3′), reverse primer (5′-TTGCTTGTCCAGGTGGTCCAT-3′), and glyceraldehyde 3-phosphate dehydrogenase: forward (5′-CCCCTGGCCAAGGTCATCCA-3′), reverse primer (5′-ACAGCCTTGGCAGCGCCAGT-3′) were used. A two-step cycling protocol on the ABI 7500 cycler was used for quantification of mRNA. Amplification parameters were as follows: initial denaturation for 10 min at 95°C, followed by 40 cycles of 15 s at 95°C and 1 min at 60°C. The relative quantification of gene expression was achieved with the $\Delta\Delta C_T$ method using manufacturer provided software.

Electrophoretic mobility shift assay

CAF cells were incubated with appropriate treatment, and nuclear lysates were prepared and processed as described (29). The consensus sequences of the oligonucleotides used were as follows: 5′-AGT TGA GGG GAC TTT CCC AGG C-3′ and 3′-TCA ACT CCC CTG AAA GGG TCC G-5′ for nuclear factor-kappaB (NF-κB), and 5′-CGC TTG ATG AGT CAG CCG GAA-3′ and 3′-GCG AAC TAC TCA GTC GGC CTT-5′ for AP-1. For the supershift assay, samples were incubated with anti-p65, anti-p50, anti-c-Jun or anti-c-Fos antibody from Santa Cruz Biotechnology (Dallas, TX). To check the specificity of DNA binding, labeled probe sample was also run together with other samples. In each case, the gel was dried and bands were visualized by autoradiography. Densitometry analysis was done using ImageJ software, and band intensities were normalized against background and expressed as fold of control value independently for each time point of the study.

TRAMPC1 allograft

Animal care and treatments were in accordance with approved Institutional guidelines and IACUC approved protocol. TRAMPC1 cells (obtained from ATCC) represent adenocarcinoma stage of the PCA and are derived from 32-week primary tumor in the prostate of PB-Tag C57BL/6 (TRAMP) mouse. These cells are tumorigenic in syngeneic C57BL/6 mice and therefore used for allograft study. Male C57Bl/6 mice were injected with 2.5×10^6 TRAMPC1 cells subcutaneously on each flank in media and Matrigel in a 1:1 ratio. Mice were orally gavaged six times a week (once daily) with silibinin (200 mg/kg body weight) or vehicle carboxymethylcellulose (0.5% w/v). The silibinin dose selected here was based on our earlier published xenograft study with DU145 cells (30) as well as a recently completed xenograft study with 22Rv1 cells (R.Agarwal *et al.*, unpublished data). In both of these studies, silibinin feeding at this dose was quite effective in reducing xenograft growth (by ≥50%) without causing any toxicity. Animal body weights were recorded weekly, and animals were monitored daily. Tumor sizes were measured biweekly using digital calipers, and tumor volume was calculated by the formula: $0.5236 \, L_1 \, (L_2)^2$, where L_1 is the long diameter, and L_2 is the short diameter. At the end, mice were killed, tumors collected and analyzed.

Immunohistochemistry

Paraffin-embedded TRAMPC1 allograft tissue sections as well as archived TRAMP PCA tissue sections from our earlier completed study were probed with anti-MCP-1, anti-F4/80, anti-CD3 and anti-Ly6g antibodies (31). In addition, TRAMPC1 sections were also incubated with anti-osteocalcin, anti-collagen I, anti-vimentin, anti-fibroblast activated protein, anti-α-smooth muscle actin and anti-transforming growth factor beta 2 (anti-TGFβ2). Most antibodies were from Abcam (Cambridge, MA), anti-osteocalcin and anti-vimentin were from Santa Cruz Biotechnology (Dallas, TX) and anti-TGFβ2 was from R&D (Minneapolis, MN). Sections were then treated with biotinylated secondary antibody (Dako, Carpinteria, CA), HRP-conjugated streptavidin, stained with 3,3′diaminobenzidene solution and counterstained with hematoxylin. Sections were analyzed by Zeiss Axioscope 2 microscope and images captured by AxioCam MrC5 camera at ×400 magnifications. Immunoreactivity (represented by brown staining) was scored as 0+ (no staining), 1+ (weak staining), 2+ (moderate staining), 3+ (strong staining) and 4+ (very strong staining).

Statistical analysis

Statistical analysis was performed using Graphpad Prism software. Data were analyzed using *t*-test, one-way analysis of variance followed by Newman–Keuls *post hoc* tests, and a statistically significant difference was considered to be at $P \leq 0.05$.

Results

Silibinin treatment reversed CCM-mediated reduction in E-cadherin expression in prostate epithelial and PCA cells

The presence of CAFs has been implicated in poor prognosis for patients of several types of cancer (14–16). Thus, we sought to identify whether CAFs play a direct role in PCA progression by inducing an invasive or aggressive phenotype in prostate epithelial and PCA cells. In parallel, we sought to identify the capacity of silibinin to target any CAF-induced activities in these cells. To accomplish these dual goals, we created a system by which CAFs would condition media which could then be applied to prostate epithelial or PCA cells. For the purposes of these studies, media conditioned with CAF in the absence or presence of silibinin was denoted as CCM and SBCM, respectively.

Our initial probe for invasive potential was the quantification of E-cadherin expression by immunofluorescence. E-cadherin is a well-established marker for epithelial cells, and conversely, useful as an inverse measure of their mesenchymal tendencies (32). As compared with basal controls, we found that exposure to CCM for 24-h reduced E-cadherin expression by 40% (*$P \leq 0.05$) in RWPE-1 cells (Figure 1A), by 50% (*$P \leq 0.05$) in WPE-1 NB-14 cells (Figure 1B), and by 21% (*$P \leq 0.05$) in PC3 cells (Figure 1C), suggesting CAFs support aggressive phenotypes in prostate/PCA cells. Addition of silibinin (CCM + SB, 50 μM) partially recovered this decrease in E-cadherin expression, by significantly (*$P \leq 0.05$) increasing E-cadherin levels over CCM treatment in all three cell types (Figure 1A–C). SBCM treatment, in turn, elicited a less dramatic reduction in E-cadherin expression as compared with CCM in RWPE-1 and NB-14 cells; however, almost no reduction in E-cadherin expression was observed in PC3 cells (Figure 1A–C). Both these findings support the notion that silibinin can inhibit the capacity of CAFs to induce a more mesenchymal phenotype on prostate epithelial/PCA cells.

Silibinin treatment reversed CCM-mediated increased invasiveness and clonogenicity in prostate epithelial and PCA cells

To investigate whether these changes in E-cadherin levels corresponded with functional changes in invasive phenotype, we next performed an invasion assay. Basal media, CCM or SBCM were placed in the bottom wells of an invasion chamber. PCA cells were seeded in the top chamber and the cells allowed to invade past a matrigel layer. CCM elicited markedly increased invasiveness in all the observed cell lines (2.5-fold, 2.8-fold and 11.2-fold in WPE-1 NA-22, WPE-1 NA-14 and PC3 cells, respectively) over basal controls, which was significantly (*$P \leq 0.05$) reduced in SBCM-treated cells (Figure 2A) confirming that CAFs can induce a significant invasive potential in PCA cells which can be inhibited by silibinin.

Clonogenicity is another measure of PCA aggressiveness. To identify whether CAFs can enhance colony formation, we performed a clonogenic assay wherein cells were seeded at very low density (~55 cells/cm²) and grown for 8 days in basal media, SBCM or CCM in the presence or absence of silibinin (50 μM). We found that CCM significantly (*$P \leq 0.05$)
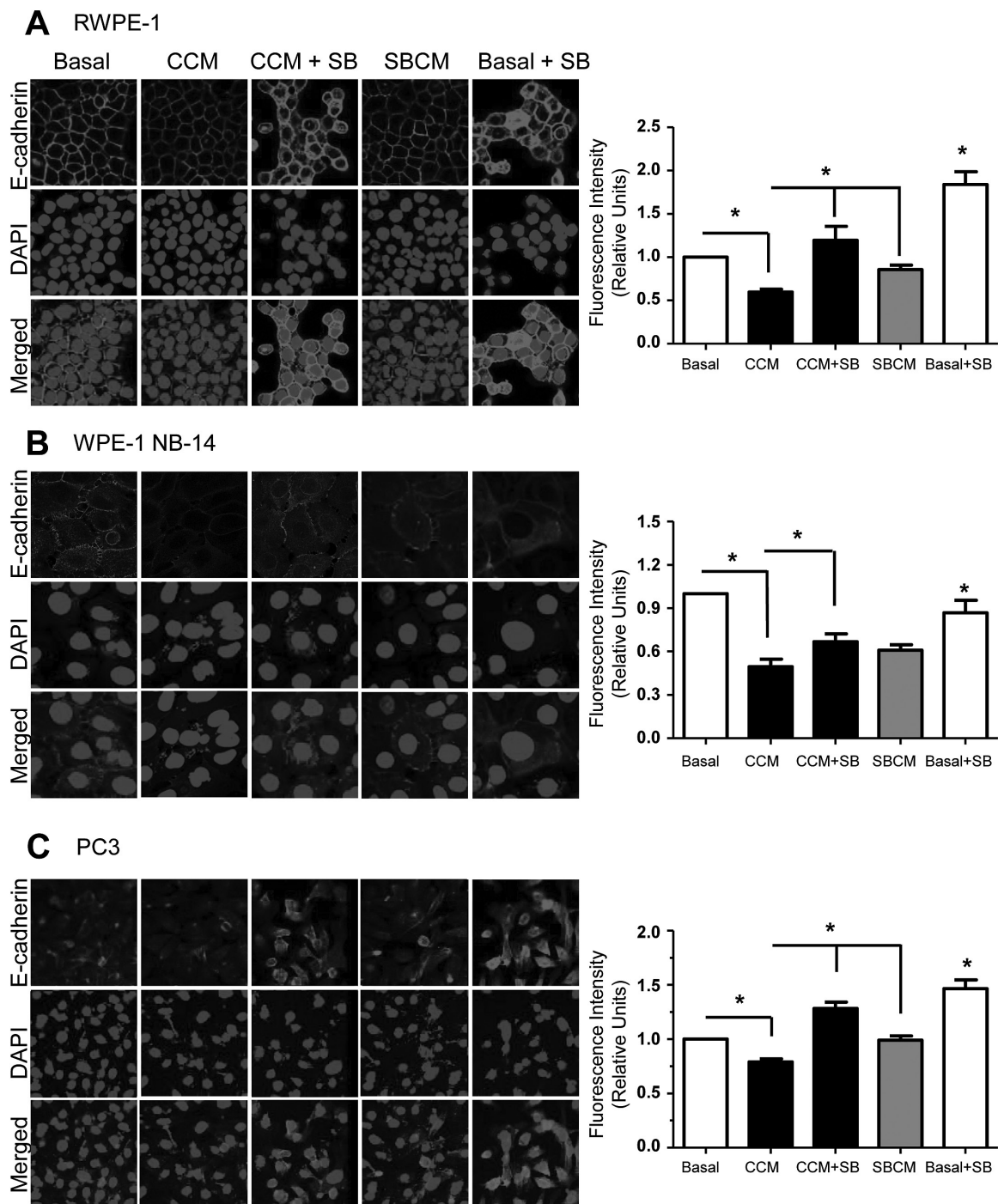
Figure 1. Characterizing the capacity of CCM to reduce E-cadherin expression. **(A)** RPWE-1, **(B)** WPE-1 NB-14 and **(C)** PC3 cells were incubated in basal media, CCM or SBCM in the presence or absence of silibinin (50 µM). After 24h, cells were analyzed for E-cadherin level (red) by immunofluorescence. Nuclei were stained with 4′,6-diamidino-2-phenylindole (blue). Immunofluorescence was quantified and normalized against cell number with data representing mean ± SEM for 10 randomly selected fields (*P ≤ 0.05).

elevated clone formation over basal controls in RWPE-1 by 26% (Figure 2B) and WPE-1 NB-14 cells by 41% (Figure 2C) but not in PC3 cells (Figure 2D). SBCM elicited colony formation roughly equivalent to basal controls, and colony formation was completely inhibited by direct application of silibinin. Thus, silibinin can act both indirectly on colony formation by inhibiting CAF-mediated clonogenicity as well as directly by inhibiting proliferation.

Silibinin treatment inhibited CCM-induced PCA invasiveness by targeting MCP-1

Having identified the capacity of CAFs to promote invasion and clone formation, we next sought to identify what secreted factors could be responsible for these phenotypic changes. We also sought to identify if the inhibitory effect of silibinin was a result of inhibiting secretion of these molecular agents. Thus, we collected CCM and SBCM from CAFs and performed a
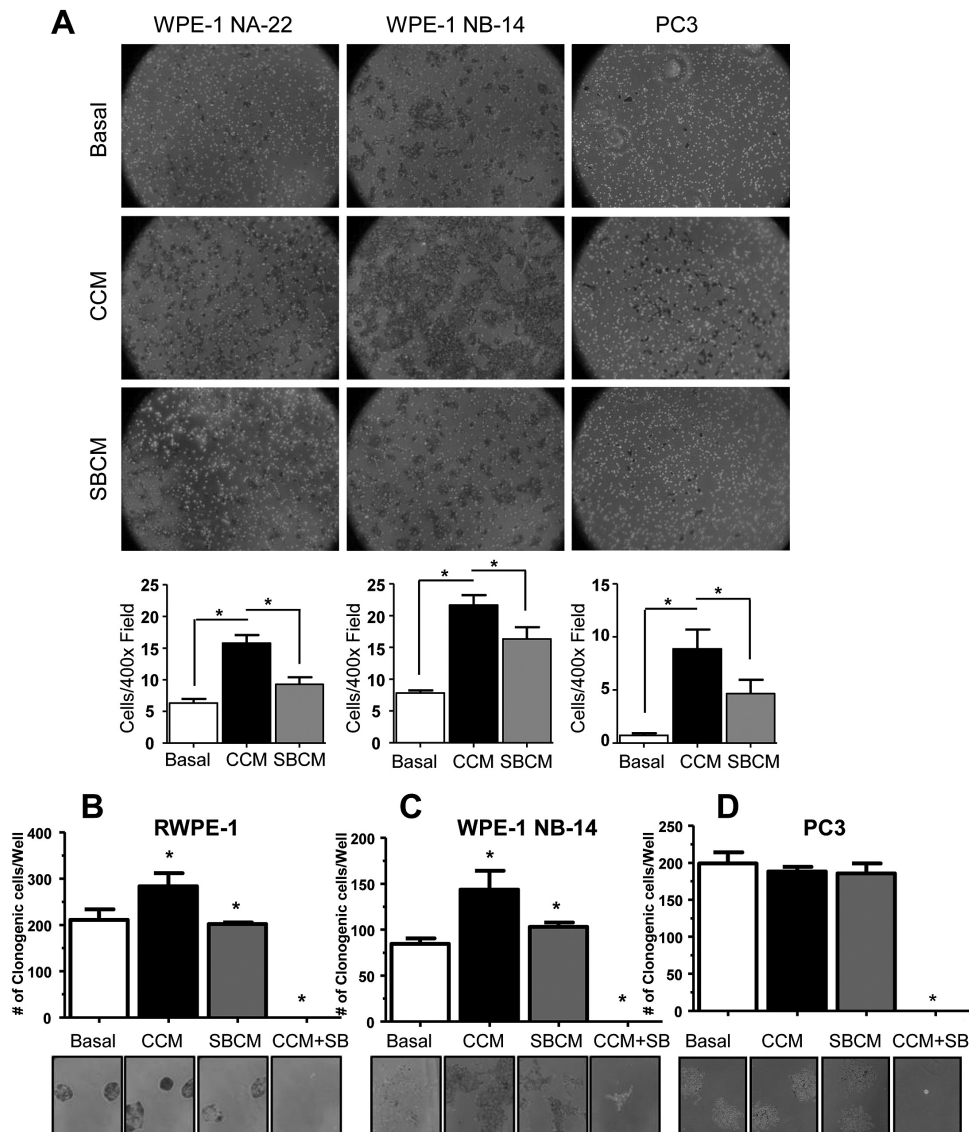
Figure 2. Investigating the capacity of CCM to increase the invasiveness and clonogenicity of PCA cells. **(A)** Basal media, CCM or SBCM were placed in the bottom wells of Trans-well invasion chambers, and WPE-1 NA-22, WPE-1 NB-14 and PC3 cells were seeded onto the top chamber. Cells were allowed to invade for 18 h and then fixed and imaged. Cells were quantified across five randomly selected fields at 400× magnification with three replicates (*P ≤ 0.05 from basal and CCM, respectively). **(B)** RWPE-1, **(C)** WPE-1 NB-14 and **(D)** PC3 cells were incubated in basal media, CCM, SBCM or CCM with silibinin (50 µM) for 8 days. Cells were then fixed and imaged for colony formation. Colonies consisting of >50 cells were counted. Data shown in bar diagram represent mean ± SEM of three samples for each group (*P ≤ 0.05).

cytokine/chemokine array. We found that CAFs potently secreted MCP-1 far in excess of other molecules (Figure 3A, CCM panels; Supplementary Figure 1 is available at *Carcinogenesis* Online), which was followed distantly by chemokine (C–X–C motif) ligand 1 (CXCL1) and macrophage migration inhibitory factor (MIF-1). Expression for all three molecules was reduced by silibinin treatment (Figure 3A, SBCM panels). The fold difference in signal between CCM and SBCM of these and other detected molecules were tabulated in Figure 3B showing a nearly 12-fold change in signal for MCP-1 between CCM and SBCM, along with more than a 3-fold change in CXCL1 and migration inhibitory factor. Other less expressed molecules that were decreased by silibinin treatment are C5/C5a, IL-1ra and IL-13 (Figure 3B). Some of the detected molecules that increased following silibinin treatment were CD154, GM-CSF and IL-6 (Figure 3B). Given its high expression, MCP-1 was further quantified by ELISA revealing that CCM contained ~3 ng of MCP-1 and SBCM ~1 ng (Figure 3C). Based on these results, we

elected to focus on the contribution of MCP-1 to the observed differences in phenotype between CCM- and SBCM-treated PCA cells.

To specifically confirm the contribution of MCP-1, we again performed an invasion assay using PC3 cells. Consistent with previous results, we found a marked induction of invasion in the presence of CCM over basal controls (Figure 3D). In addition, basal media supplemented with exogenous MCP-1 to levels found in our MCP-1 ELISA of CCM (3 ng) elicited almost as much invasion in PC3 cells as CCM itself. SBCM, consistent with its lower levels of MCP-1 (1 ng) elicited lower levels of invasion, and consistent with our previous finding, basal media supplemented with similar levels of MCP-1 (1 ng) as SBCM elicited almost as much invasion. Importantly, SBCM supplemented with exogenous MCP-1 to the level of CCM (1 ng from SBCM, 2 ng exogenously added, 3 ng total) induced almost as much invasiveness as CCM.

To further confirm the role of MCP-1, we performed invasion assay with the addition of specific neutralizing antibodies to
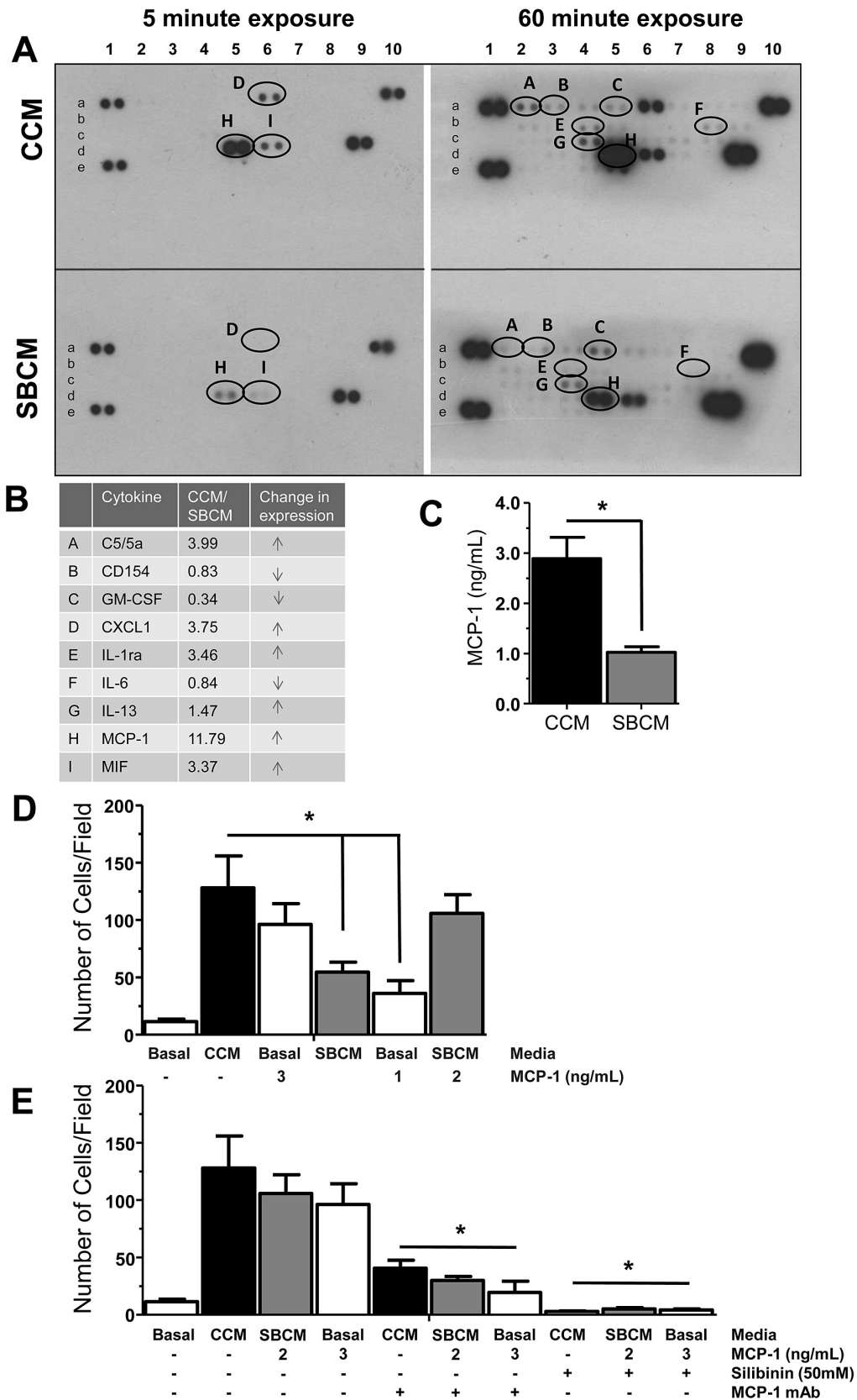
Figure 3. Characterizing the role of MCP-1 in CCM-mediated PCA cell invasiveness. CCM and SBCM were collected and then assayed by cytokine array (**A** and **B**) and ELISA (**C**). Data shown in bar diagrams represent mean ± SEM of three samples for each group (*P ≤ 0.05). (**D**) PC3 cells were seeded onto invasion chambers (25 000 cells/well) in wells containing basal media (control), CCM or SBCM with or without MCP-1 (1–3 ng/ml). (**E**) Specific MCP-1-neutralizing antibodies were added to wells containing CCM, SBCM + MCP-1, and basal + MCP-1. Silibinin (50 μM) was added to wells containing CCM, SBCM + MCP-1, and basal + MCP-1. Cells were quantified across 10 randomly selected fields at ×100 magnification with 3 replicates (*P ≤ 0.05).

MCP-1 (Figure 3E). We report a significant reduction (*$P \leq 0.05$) in PC3 invasion upon addition of these antibodies confirming the role of MCP-1 in CAF mediated invasion (Figure 3E). Furthermore, addition of silibinin (50 μM) directly, nearly completely abrogated PC3 invasion, confirming silibinin's capacity to inhibit PCA response to CAF-mediated invasion.

Silibinin treatment reduced MCP-1 transcription via inhibiting the DNA binding of NF-κB and AP-1 transcription factors

Next, we sought to elucidate the mechanism by which silibinin inhibited CAF secretion of MCP-1. We first sought to identify if the reduced concentration of MCP-1 found in SBCM versus CCM was a direct result of reduced synthesis of MCP-1 by silibinin treatment. We observed a 2-fold (*$P \leq 0.05$) decrease in MCP-1 mRNA in silibinin-treated CAF cells versus control by 12 h, which reached a maximum of a 4-fold reduction by 48 h (Figure 4A; Supplementary Figure 2 is available at *Carcinogenesis* Online). To further characterize the mechanism of silibinin-mediated inhibition of MCP-1 expression, we next analyzed the signaling in CAFs upstream of MCP-1 transcription. Accordingly, we collected nuclear lysates of control and silibinin-treated CAF cells and analyzed them by electrophoretic mobility shift assay and supershift assay for NF-κB and AP-1, known transcriptional regulators of MCP-1 (33–35). Here, our electrophoretic mobility shift assay revealed a notable reduction in NF-κB and AP-1 activation in silibinin-treated (90 μM) CAF versus controls (Figure 4B and C). Our supershift assay reveals that p50 and c-jun were much more significant components of the total NF-κB and AP-1 complexes, respectively (Figure 4D).

Silibinin feeding reduced TRAMPC1 allograft growth via decreasing MCP-1, CAFs activation and immune cells recruitment

Spurred by these findings, we elected to examine this model of PCA progression *in vivo*, taking TRAMPC1 cells derived from transgenic adenocarcinoma of the mouse prostate (TRAMP) mice and injecting them into syngeneic C57Bl/6 mice. Importantly, this approach provided an immune competent background to investigate the contribution of MCP-1 on immune cell recruitment as well as the effect of silibinin on this interaction. Mice were treated by oral gavage with vehicle control or silibinin, and at the end of the study, we found that both tumor volume and mass were significantly (*$P \leq 0.05$) reduced by silibinin treatment over control (55 and 68%, respectively) (Figure 5A–B). Tumor growth and silibinin treatment had no effect on mouse weight throughout the study (data not shown).

Allografts were then collected and processed by immunohistochemistry (Figure 5C). Consistent with our *in vitro* data, MCP-1 accumulation was significantly (*$P \leq 0.05$) reduced as compared with control, and consistent with its normally ascribed immune function, this corresponded to a reduction in infiltration by macrophages (F4/80) (36). In addition, we also noted a significant (*$P \leq 0.05$) reduction in neutrophils (Ly6g), but not T cells (CD3) in silibinin-treated mice as compared with controls, which is also consistent with data shown in Figure 4B revealing a marked reduction in CXCL1, a potent neutrophil chemokine (37) in SBCM compared with CCM. Interestingly, upon sacrifice and tumor collection, we found that these tumors were quite hard, perhaps a sign of fibrosis or even bone formation. Thus, we analyzed them for the bone precursor molecule, osteocalcin and the presence of collagen I. We noted an extensive amount of both in tumors of control mice that was significantly (*$P \leq 0.05$) reduced in silibinin-treated mice (Figure 5D), suggesting decreased activity in

their CAFs as well as osteoblasts. To further confirm the presence of activated, CAFs, we assayed for the presence of CAF markers, α-smooth muscle actin, fibroblast activation protein and vimentin, as well as TGFβ2, a molecule we recently investigated as an activator of naive human fibroblasts (17). We found extensive amounts of all four molecules in tumors from control mice, which were significantly (*$P \leq 0.05$) reduced in the tumors from silibinin-treated mice (Figure 5D).

Silibinin feeding of TRAMP mice inhibited MCP-1 expression in prostate tumors which corresponded to a reduction in immune cell infiltration

To further confirm our findings in a tumor system that closely follows clinical presentation of PCA in humans, we assayed archived samples from a previously completed study performed in the TRAMP mouse model (31). This model is both immune competent and most importantly spontaneously forms prostate tumors unlike most mouse models. In this study, TRAMP mice (at age 12 weeks) were given control or 1% silibinin supplemented diet for 8 weeks whereupon they were sacrificed at 20 weeks of age. Prostate tumors from TRAMP mice were collected and analyzed. Silibinin-fed TRAMP mice exhibited significantly less pathological score and disease advancement (in terms of PIN, adenocarcinoma and metastasis), which corresponded to a reduction in biomarkers for proliferation, angiogenesis and invasion (31). In the present study, TRAMP prostate tissues were further analyzed by immunohistochemistry for MCP-1 and immune cells biomarkers. Consistent with our other results, silibinin treatment significantly reduced the MCP-1 expression (Figure 6A), which was associated with a reduction in F4/80 (Figure 6B) and Ly6g (Figure 6C) but without any significant change in CD3 expression (Figure 6D).

Discussion

The tumor microenvironment plays a central role at each stage of carcinogenesis. Both the stromal fibroblasts surrounding a tumor and the immune cells infiltrating a tumor might be expected to act as tumor suppressors. Stromal fibroblasts encapsulate and physically constrain the growth of a tumor, whereas leukocytes maintain immune surveillance, eliminating or stunting the growing tumor (27). There appears to be a stage where these previously tumor suppressive elements transition into becoming tumor permissive, and even tumor supportive. The development of CAFs has been recently recognized as an indicator of poor prognosis, and efforts have been made to characterize the actions and mechanisms through which they support tumor progression (14–16). Likewise, the contribution to tumor progression of an inflammatory background associated with chronic leukocyte recruitment has been well established (4,27). Therefore, these cellular components of the tumor microenvironment offer novel opportunities to prevent and/or treat cancer.

In a previous study, we identified the capacity of PCA cells to induce a CAF-like phenotype in naive fibroblasts (17). Here, we found that CAFs could increase the clonogenicity and invasiveness of PCA cells. This suggests a cycle whereby PCA recruits/induces CAFs to support PCA invasiveness, which promotes its expansion into new tissues where it can again recruit/induce more CAFs, ultimately increasing the pool of PCA cells that escape cellular barriers to begin metastasis, a critical stage in cancer-related mortality. In addition, we identified that MCP-1 is the principal agent driving this response, though other chemokines such as CXCL1 and macrophage migration inhibitory factor are also detected in CCM. Consistent with the
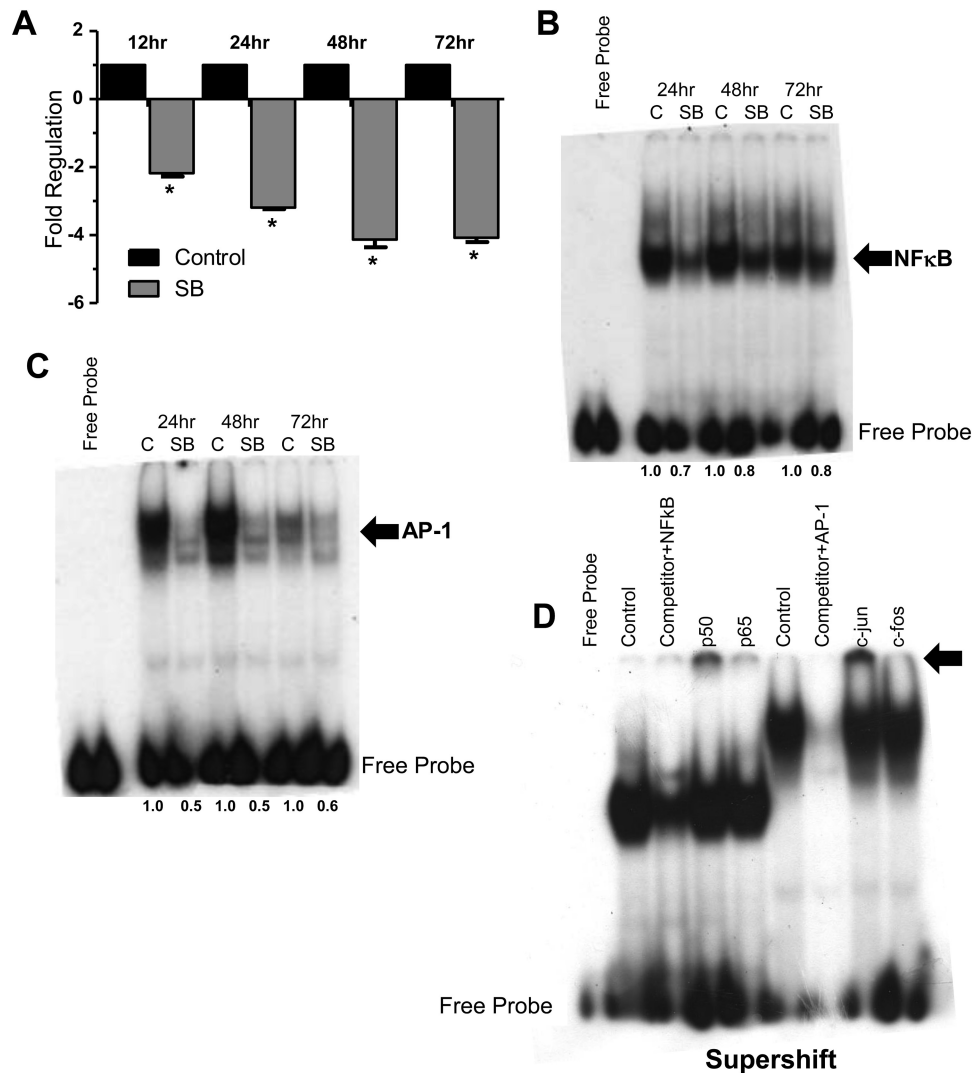
Figure 4. Silibinin inhibits MCP-1 transcript level as well as DNA binding of transcriptional regulators of MCP-1 in CAFs. CAFs were incubated in basal media in the presence or absence of silibinin (90 μM) for the indicated times. **(A)** At the end of each time point, cells were collected and total RNA isolated. Real-time PCR was performed to measure silibinin effect on MCP-1 mRNA as detailed in Methods. Data were normalized against glyceraldehyde 3-phosphate dehydrogenase (*P ≤ 0.05). **(B–D)** Nuclear lysates were collected and analyzed by EMSA and supershift assay to define silibinin (90 μM) effect on MCP-1 transcriptional regulators NF-κB and AP-1 after 24–72 h of treatment. Gels cropped for clarity. Densitometry values, shown under the gels in panels (B) and (C), were determined by normalizing band intensities against background and expressed as fold of control values independently for each time point of the study.

typically assigned role of MCP-1 and other chemokines, we found that immune cells were recruited to both TRAMPC1 allografts as well as prostate tumors in TRAMP mice. Interestingly, we reported previously that PCA cells secrete TGFβ2. TGFβ isoforms have typically been identified as tumor suppressive. However, in a situation similar to that of cancer associated immune cells and fibroblasts described previously, TGFβ becomes adapted by aggressive cancer cells to instead induce tumor cell epithelial-mesenchymal transition (38). Additionally, and in light of the present work perhaps most importantly, TGFβ also serves to inhibit immune surveillance by natural killer and cytotoxic T cells (39). This suggests a multifaceted activity whereby PCA cells secrete TGFβ isotypes to recruit/induce CAFs, which in turn secrete MCP-1 and other chemokines to recruit immune cells, after which resident TGFβ inhibits cytotoxic T-cell and natural killer activity while allowing for other immune cell mediated activities (particularly the establishment of a chronic inflammatory background along with immunosuppression) that have

been reported to support tumor cell proliferation and metastasis while reducing apoptosis (5).

In addition to these findings, we report that application of the flavonolignan, silibinin, inhibited CAF-mediated promotion of invasiveness in PCA cells as well as inhibited tumor growth, fibroblast activation and immune cell recruitment *in vivo*. Our results were consistent with silibinin's established effects directly inhibiting epithelial-mesenchymal transition, migration and invasion in PCA cells as well as actions related to the tumor microenvironment such as inhibiting angiogenesis (20,21,31,40). In this context, we had previously investigated the ability of silibinin to target PCA-mediated alteration of naive human prostate fibroblasts into a CAF-like phenotype, finding that silibinin could indeed target this early dysfunction of the cellular microenvironment brought on by PCA cells (17). This suggests a broad role for silibinin regarding the prostate tumor microenvironment. It can target the upstream event of an incipient lesion recruiting fibroblasts to drive further dysfunction. It
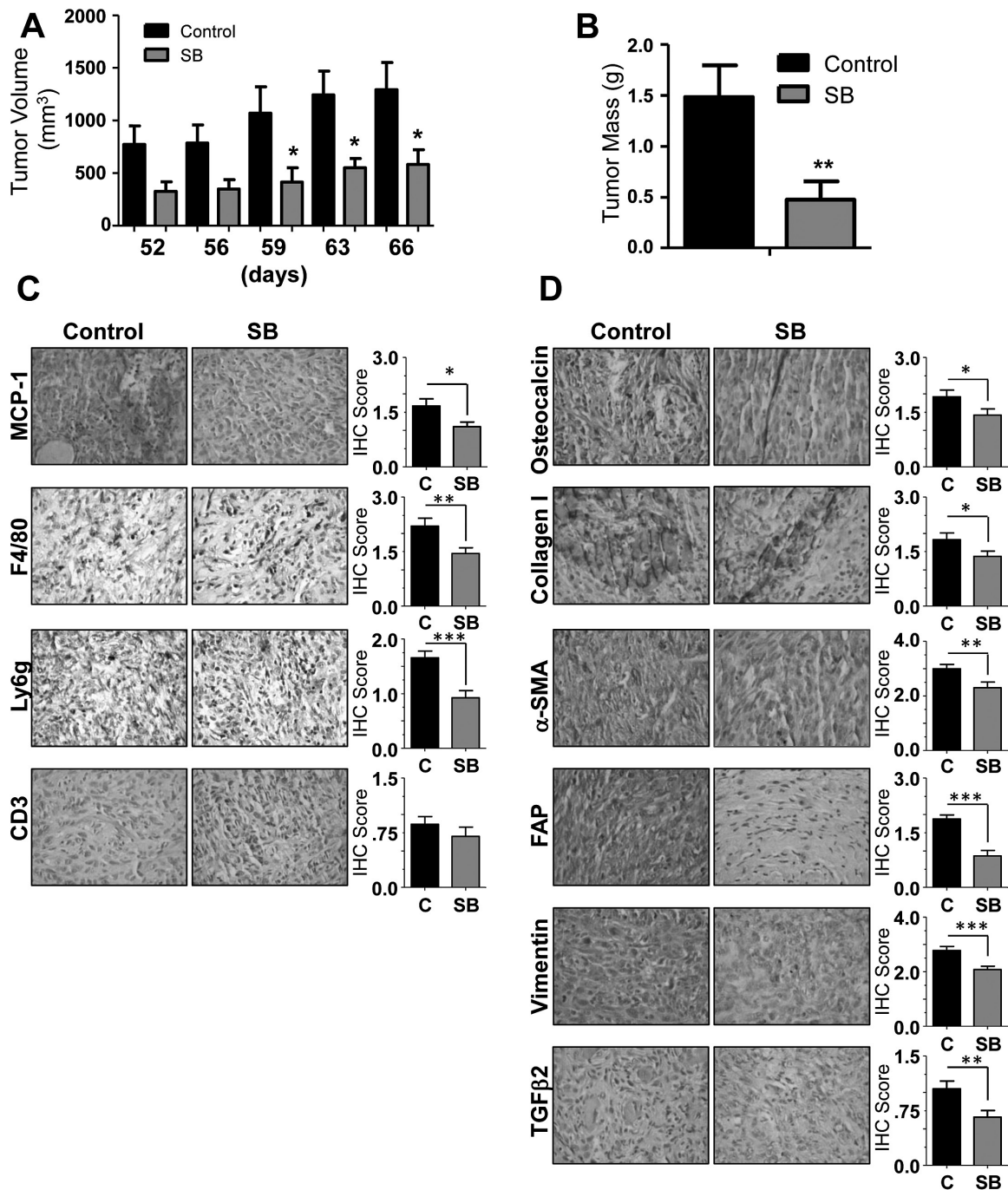
Figure 5. Silibinin feeding inhibits TRAMPC1 allograft growth in C57Bl/6 mice via targeting immune cells recruitment, bone precursor molecules and activated fibroblast. Male C57Bl/6 mice were injected subcutaneously with 2.5×10^6 million TRAMPC1 cells in each flank and treated six times a week (once daily) with silibinin (200 mg/kg body weight) or vehicle (0.5% CMC) for 66 days. **(A)** Tumor volume was measured as described in Methods. **(B)** Tumor mass was determined upon mouse sacrifice (*$P \leq 0.05$; **$P \leq 0.01$). **(C and D)** Allografts were collected, sectioned and analyzed by immunohistochemistry for MCP-1, F4/80, Ly6g, CD3, osteocalcin, collagen I, α-smooth muscle actin, fibroblast activation protein, vimentin and TGFβ2. Data shown in bar diagrams represent mean ± SEM of immunoreactivity scores for 10 randomly selected 400× fields/sample from 3 samples for each group (*$P \leq 0.05$; **$P \leq 0.01$; ***$P \leq 0.005$).

can inhibit the downstream event of these now constitutively activated fibroblasts acting to promote PCA cell invasion. It can also prevent CAFs ability to promote immune cell infiltration, while also inhibiting tumor angiogenesis. These effects are in addition to silibinin's well-documented ability to directly rescue dysfunctional cell signaling in PCA (18,19,41), reducing proliferation and promoting apoptosis (19,20,42). Together, these results point to the potential of silibinin to serve as a novel agent in

PCA management via targeting cancer cells, tumor microenvironment components and interactions between the two.

This is important as PCA remains a pressing issue. In spite of notable investment and success in improving early detection, it remains the second leading cause for cancer-related mortality among American men (43). Additionally, autopsy studies reveal a significant incidence of undetected PCA in patients and notable amounts in patients much younger than typically expected,
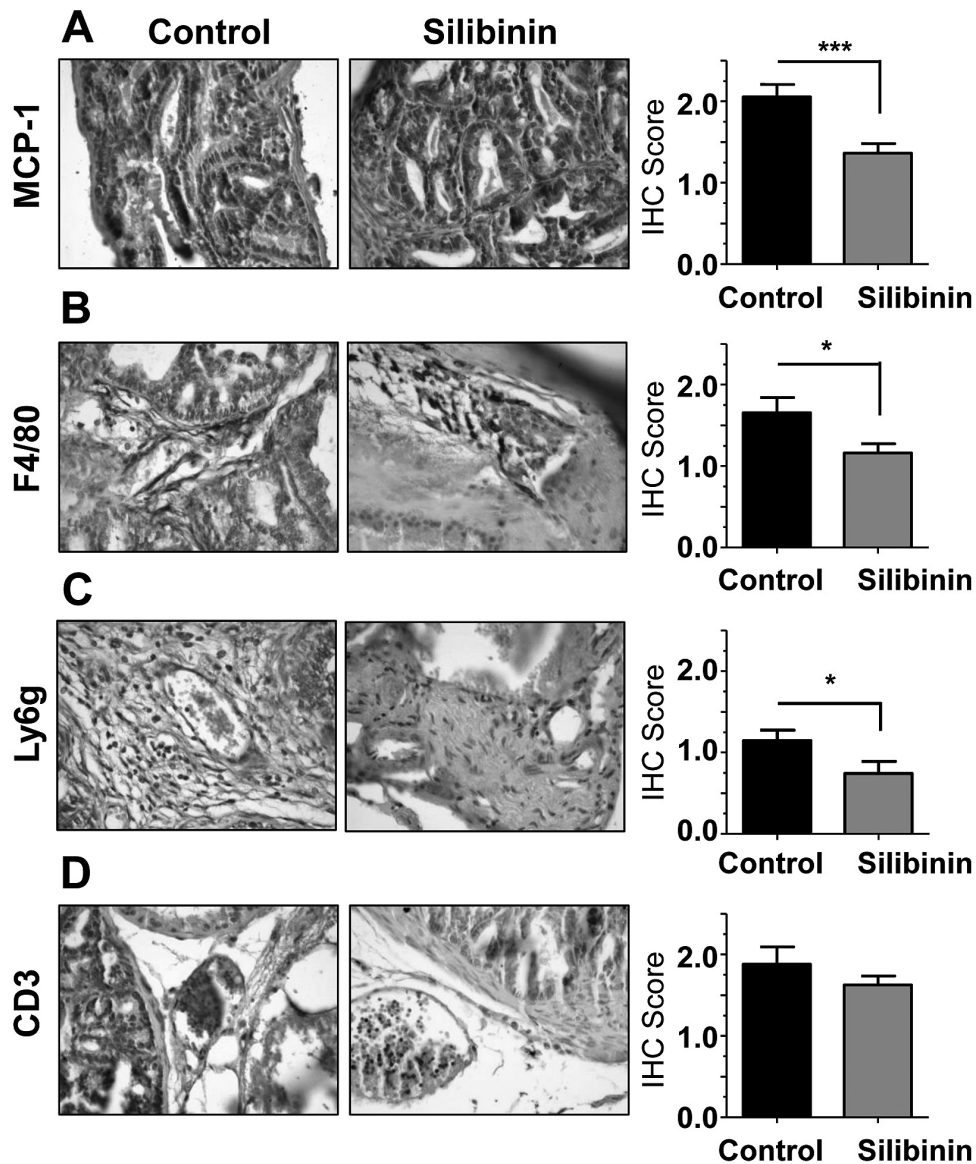
Figure 6. Effect of silibinin feeding on MCP-1 expression and immune cell recruitment to the sites of PCA in TRAMP mice. Prostate tissues from control or silibinin-fed TRAMP mice were analyzed by immunohistochemistry for **(A)** MCP-1, **(B)** F4/80, **(C)** Ly6g and **(D)** CD3. Data shown in bar diagrams represent mean ± SEM of immunoreactivity scores for 10 randomly selected 400× fields/sample from 3 samples for each group (*P ≤ 0.05; ***P ≤ 0.005).

suggesting these diagnostic efforts may still fall short of completely effective screening (44). Together, these data highlight two related needs: the development of novel agents targeting aspects of the disease that may currently be unaddressed and the development of agents that can serve as long-term prophylaxis prior to any specific diagnosis of PCA. Importantly, silibinin is a natural product, taken for millennia as the main active ingredient in milk thistle for treatment of several disorders. As such, it has been shown to be well tolerated and of low toxicity, preferable properties for any long-term intervention, and perhaps even making silibinin suitable for use prior to diagnosis of PCA. To that end, and in light of silibinin's ability to target both PCA cells directly and to inhibit the dysfunctional activities within the tumor microenvironment that have been identified as critical for the support and progression of a tumor, silibinin has been investigated in phase I/II clinical trials in PCA patients (45,46). Dose-escalation studies confirmed that concentrations of silibinin used in our cell culture studies were physiologically achievable in the plasma of PCA patients (46).

For the purposes of the present study, there remains a concern that silibinin treatment reduced the size of tumors, and thus any observed changes in marker levels might be related to changes in tumor volume rather than specific inhibition of CAF activity and/or immune cells recruitment. As a consequence, an experiment where tumors are collected at sequential times (and thus predicted to be of increasing sizes) might be needed to address this concern. Further studies will also be needed to specifically address the contribution of MCP-1 *in vivo*, particularly in regards to tumor growth and immune cell recruitment. These will involve the use of MCP-1 KO mice and syngeneic mouse CAF and TRAMPC1 cells. These mice provide a background incapable of secreting MCP-1, whereas injected CAFs would be expected to provide this agent with the TRAMPC1 cells being the tumorigenic cell line used in the present study. Taken together, we identified a role for CAFs in mediating PCA dysfunction through the secretion of MCP-1 and identified the capacity of silibinin to inhibit this phenomenon, both as a direct action on CAF secretion of

MCP-1 and directly inhibiting PCA activity in response to exposure to CAF conditioned media.

Supplementary material

Supplementary Figures 1 and 2 can be found at http://carcin.oxfordjournals.org/

Funding

References

1. Armitage, P. et al. (1954) The age distribution of cancer and a multi-stage theory of carcinogenesis. Br. J. Cancer, 8, 1–12.
2. Albini, A. et al. (2007) The tumour microenvironment as a target for chemoprevention. Nat. Rev. Cancer, 7, 139–147.
3. Huang, L. et al. (2014) Cancer-associated fibroblasts in digestive tumors. World J. Gastroenterol., 20, 17804–17818.
4. Quail, D.F. et al. (2013) Microenvironmental regulation of tumor progression and metastasis. Nat. Med., 19, 1423–1437.
5. Hanahan, D. et al. (2012) Accessories to the crime: functions of cells recruited to the tumor microenvironment. Cancer Cell, 21, 309–322.
6. Pietras, K. et al. (2010) Hallmarks of cancer: interactions with the tumor stroma. Exp. Cell Res., 316, 1324–1331.
7. Fang, H. et al. (2013) Targeting the tumor microenvironment: from understanding pathways to effective clinical trials. Cancer Res., 73, 4965–4977.
8. Jemal, A. et al. (2010) Global patterns of cancer incidence and mortality rates and trends. Cancer Epidemiol. Biomark. Prev., 19, 1893–1907.
9. Goetz, J.G. (2012) Tumor microenvironment indoctrination: an emerging hallmark of cancer. Cell Adhes. Migr., 6, 190–192.
10. McAnulty, R.J. (2007) Fibroblasts and myofibroblasts: their source, function and role in disease. Int. J. Biochem. Cell Biol., 39, 666–671.
11. Kendall, R.T. et al. (2014) Fibroblasts in fibrosis: novel roles and mediators. Front. Pharmacol., 5, 123.
12. Cirri, P. et al. (2011) Cancer associated fibroblasts: the dark side of the coin. Am. J. Cancer Res., 1, 482–497.
13. Kakarla, S. et al. (2012) Cancer-associated fibroblasts as targets for immunotherapy. Immunotherapy, 4, 1129–1138.
14. Underwood, T.J. et al. (2015) Cancer-associated fibroblasts predict poor outcome and promote periostin-dependent invasion in oesophageal adenocarcinoma. J. Pathol., 235, 466–477.
15. Saigusa, S. et al. (2011) Cancer-associated fibroblasts correlate with poor prognosis in rectal cancer after chemoradiotherapy. Int. J. Oncol., 38, 655–663.
16. Cheng, Y. et al. (2015) Cancer-associated fibroblasts are associated with poor prognosis in esophageal squamous cell carcinoma after surgery. Int. J. Clin. Exp. Med., 8, 1896–1903.
17. Ting, H.J. et al. (2015) Silibinin prevents prostate cancer cell-mediated differentiation of naïve fibroblasts into cancer-associated fibroblast phenotype by targeting TGF β2. Mol. Carcinog., 54, 730–741.
18. Dhanalakshmi, S. et al. (2002) Silibinin inhibits constitutive and TNFalpha-induced activation of NF-kappaB and sensitizes human prostate carcinoma DU145 cells to TNFalpha-induced apoptosis. Oncogene, 21, 1759–1767.
19. Agarwal, C. et al. (2007) Silibinin inhibits constitutive activation of Stat3, and causes caspase activation and apoptotic death of human prostate carcinoma DU145 cells. Carcinogenesis, 28, 1463–1470.
20. Singh, R.P. et al. (2003) Suppression of advanced human prostate tumor growth in athymic mice by silibinin feeding is associated with reduced cell proliferation, increased apoptosis, and inhibition of angiogenesis. Cancer Epidemiol. Biomark. Prev., 12, 933–939.
21. Deep, G. et al. (2011) Role of E-cadherin in antimigratory and antiinvasive efficacy of silibinin in prostate cancer cells. Cancer Prev. Res. (Phila.), 4, 1222–1232.
22. Chang, H.R. et al. (2011) Silibinin inhibits the invasion and migration of renal carcinoma 786-O cells *in vitro*, inhibits the growth of xenografts
23. Noh, E.M. (2011) Silibinin enhances ultraviolet B-induced apoptosis in mcf-7 human breast cancer cells. J. Breast Cancer, 14, 8–13.
24. Singh, R.P. et al. (2006) Silibinin inhibits UVB- and epidermal growth factor-induced mitogenic and cell survival signaling involving activator protein-1 and nuclear factor-kappaB in mouse epidermal JB6 cells. Mol. Cancer Ther., 5, 1145–1153.
25. Nambiar, D.K. et al. (2014) Silibinin inhibits aberrant lipid metabolism, proliferation and emergence of androgen-independence in prostate cancer cells via primarily targeting the sterol response element binding protein 1. Oncotarget, 5, 10017–10033.
26. Jiang, K. et al. (2015) Silibinin, a natural flavonoid, induces autophagy via ROS-dependent mitochondrial dysfunction and loss of ATP involving BNIP3 in human MCF7 breast cancer cells. Oncol. Rep., 33, 2711–2718.
27. Zamarron, B.F. et al. (2011) Dual roles of immune cells and their factors in cancer development and progression. Int. J. Biol. Sci., 7, 651–658.
28. Kavitha, C.V. et al. (2014) Silibinin inhibits prostate cancer cells- and RANKL-induced osteoclastogenesis by targeting NFATc1, NF-κB, and AP-1 activation in RAW264.7 cells. Mol. Carcinog., 53, 169–180.
29. Chittezhath, M. et al. (2008) Silibinin inhibits cytokine-induced signaling cascades and down-regulates inducible nitric oxide synthase in human lung carcinoma A549 cells. Mol. Cancer Ther., 7, 1817–1826.
30. Deep, G. et al. (2008) Isosilibinin inhibits advanced human prostate cancer growth in athymic nude mice: comparison with silymarin and silibinin. Int. J. Cancer, 123, 2750–2758.
31. Raina, K. et al. (2008) Stage-specific inhibitory effects and associated mechanisms of silibinin on tumor progression and metastasis in transgenic adenocarcinoma of the mouse prostate model. Cancer Res., 68, 6822–6830.
32. Lamouille, S. et al. (2014) Molecular mechanisms of epithelial-mesenchymal transition. Nat. Rev. Mol. Cell Biol., 15, 178–196.
33. Martin, T. et al. (1997) Cytokine induction of monocyte chemoattractant protein-1 gene expression in human endothelial cells depends on the cooperative action of NF-kappa B and AP-1. Eur. J. Immunol., 27, 1091–1097.
34. Deng, X. et al. (2013) Transcriptional regulation of increased CCL2 expression in pulmonary fibrosis involves nuclear factor-κB and activator protein-1. Int. J. Biochem. Cell Biol., 45, 1366–1376.
35. Panee, J. (2012) Monocyte chemoattractant protein 1 (MCP-1) in obesity and diabetes. Cytokine, 60, 1–12.
36. Deshmane, S.L. et al. (2009) Monocyte chemoattractant protein-1 (MCP-1): an overview. J. Interferon Cytokine Res., 29, 313–326.
37. De Filippo, K. et al. (2013) Mast cell and macrophage chemokines CXCL1/CXCL2 control the early stage of neutrophil recruitment during tissue inflammation. Blood, 121, 4930–4937.
38. Xu, J. et al. (2009) TGF-beta-induced epithelial to mesenchymal transition. Cell Res., 19, 156–172.
39. Hanahan, D. et al. (2011) Hallmarks of cancer: the next generation. Cell, 144, 646–674.
40. Wu, K. et al. (2010) Silibinin reverses epithelial-to-mesenchymal transition in metastatic prostate cancer cells by targeting transcription factors. Oncol. Rep., 23, 1545–1552.
41. Tyagi, A. et al. (2008) Silibinin impairs constitutively active TGFalpha-EGFR autocrine loop in advanced human prostate carcinoma cells. Pharm. Res., 25, 2143–2150.
42. Tyagi, A. et al. (2002) Antiproliferative and apoptotic effects of silibinin in rat prostate cancer cells. Prostate, 53, 211–217.
43. Lewis, D.R. et al. (2015) Early estimates of SEER cancer incidence for 2012: approaches, opportunities, and cautions for obtaining preliminary estimates of cancer incidence. Cancer, 121, 2053–2062.
44. Sakr, W.A. et al. (1993) The frequency of carcinoma and intraepithelial neoplasia of the prostate in young male patients. J. Urol., 150 (2 Pt 1), 379–385.
45. Flaig, T.W. et al. (2010) A study of high-dose oral silybin-phytosome followed by prostatectomy in patients with localized prostate cancer. Prostate, 70, 848–855.
46. Flaig, T.W. et al. (2007) A phase I and pharmacokinetic study of silybin-phytosome in prostate cancer patients. Invest. New Drugs, 25, 139–146.